Dielectric behaviour and phase transition of $SrAlF_5$ single crystals

2006 J. Phys.: Condens. Matter 18 2511

(http://iopscience.iop.org/0953-8984/18/8/014)

INSTITUTE OF PHYSICS PUBLISHING JOURNAL OF PHYSICS: CONDENSED MATTER

J. Phys.: Condens. Matter **18** (2006) 2511–2523 doi:10.1088/0953-8984/18/8/014

Dielectric behaviour and phase transition of $SrAlF_5$ single crystals

E N Silva[1], A P Ayala[1,2], R L Moreira[3] and J-Y Gesland[4]

[1] Departamento de Física, Universidade Federal do Ceará, Caixa Postal 6030, 60455-900, Fortaleza, Ceará, Brazil
[2] Department of Physical Chemistry, University of Duisburg-Essen, Essen D45117, Germany
[3] Departamento de Física, ICEx, Universidade Federal de Minas Gerais, Caixa Postal 702, 30123-970, Belo Horizonte, Minas Gerais, Brazil
[4] Université du Maine-Cristallogénèse, UMR 6087, 72085 Le Mans Cedex 9, France

E-mail: eder@fisica.ufc.br (E N Silva)

Received 22 August 2005, in final form 16 January 2006
Published 10 February 2006
Online at stacks.iop.org/JPhysCM/18/2511

Abstract

Dielectric constant and ionic conductivity measurements have been performed in $SrAlF_5$ single crystals, along the [100] and [001] directions, as functions of frequency (10 Hz–10 MHz) and temperature (300–800 K). The real part of the *ac* conductivity showed the 'universal dynamic response of dielectrics', evidenced by a power-law dependency on the frequency. A first-order phase transition was observed around 715 K, with a considerable thermal hysteresis in the real part of the dielectric constant and in the electrical conductivity. The ionic conductivity varies by about four orders of magnitude in the temperature interval studied and shows various regions with Arrhenius behaviour with activation energies ranging from 0.2 to 1.40 eV.

1. Introduction

Fluoride crystals have been considered promising candidates for solid-state laser hosts due to their remarkable optical properties, including high transparency, low cut-off phonon energies and high resistance to optical damage. Several authors have reported on the optical properties of $SrAlF_5$ when used as a host for rare earth and transition metal active ions. Indeed, it was verified that Cr^{3+} and Ce^{3+} doped $SrAlF_5$ exhibit wide emission bands in the spectral range from infrared to ultraviolet [1–3], being suitable for building up solid-state tunable lasers. In order to improve the knowledge of the optical and spectroscopic characteristics of the doped crystals, $SrAlF_5$:Cr^{3+} crystals were investigated by electron paramagnetic resonance [4] and time-resolved Z-scan and thermal lens techniques [5]. On the other hand, the emission spectra of Pr^{3+} doped crystals were recorded, allowing the observation of phonon cascade emission processes in the infrared and visible spectral ranges [6, 7]. Since alkaline earth sites are adequate for doping with divalent active ions, like Eu^{2+} [8–10], $SrAlF_5$ offers the possibility of

co-doping the crystal with active ions emitting in the visible and ultraviolet spectral regions, as was shown by van der Kolk *et al* [11]. $SrAlF_5$, which has been shown to be transparent between 0.16 and 10 μm approximately [10, 12], has recently become one of the most promising candidates for the realization of solid-state lasers in the ultraviolet wavelength region by the quasi-phase-matching technique [13].

$SrAlF_5$ has been cited several times as one of the rare crystalline fluorides that exhibit ferroelectricity at room temperature [14–16]. The origin of the spontaneous polarization was predicted using the Abrahams–Kurtz–Jamieson (AKJ) theory [17], which correlates the Curie temperature with the atomic displacements between the paraelectric and ferroelectric crystalline structures. In the special case of the $MAlF_5$ (M = Sr, Ca, Ba) family, Abrahams *et al* [18, 19], based on the crystalline structure reported by von der Mühll *et al* [20], applied the AKJ theory to predict a ferroelectric phase transition at 685 K in $SrAlF_5$. These authors confirmed the existence of a phase transition by observing anomalies in the dielectric constant and specific heat of polycrystalline samples at about 715 K. Supporting these results, Canouet *et al* [21] have also observed a phase transition at the same temperature in the crystal optical birefringence. Even though the experimental data supported the existence of a high-temperature phase transition in $SrAlF_5$, it was in a recent work that Shimamura *et al* [12, 13] reported direct evidences that should support the ferroelectric character of $SrAlF_5$ by presenting measures of polarization hysteresis loops. However, these results are not conclusive since the coercive field was not determined and the hysteresis loops are strongly dependent on the applied field, exhibiting a rounded shaped possibly due to the presence of an electrical current component. On the other hand, Kubel [22] presented a single-crystal x-ray diffraction study of $SrAlF_5$ and proposed a tetragonal structure at room temperature, belonging to the $I4_1/a$ space group. The presence of an inversion centre in the $I4_1/a$ space group forbids ferroelectricity in this compound. In a recent work, the existence of an inversion centre in $SrAlF_5$ was investigated using polarized Raman and infrared spectroscopies [23]. These results suggest a centrosymmetric crystalline system, but the reduced number of observed vibrational bands is best described by a smaller unit cell being a substructure of the one proposed by Kubel. Several authors reported to have observed second harmonic generation (SHG) in $SrAlF_5$ [12, 13, 18, 19], but all of these measurements were performed in powder samples, where SHG may be induced by extrinsic effects. On the other hand, several attempts to observe SHG or electrooptical modulation in high-quality single crystals gave negative results.

Despite the large number of works dealing with the optical, structural and thermal properties of $SrAlF_5$, several discrepancies can easily be identified when comparing these results. In order to contribute to their understanding, in this work, the electric and dielectric properties of $SrAlF_5$ single crystals have been investigated by impedance spectroscopy. Temperature-dependent measurements (300–800 K) have been performed along the [100] and [001] crystallographic directions, for frequencies varying between 10 Hz and 10 MHz. Our results exhibit evidences of a first-order structural phase transition, in agreement with previous reports. Moreover, strong irreversible effects were observed in both dielectric constant and conductivity results. This behaviour is discussed in terms of the possible conduction pathways in the crystal structure.

2. Experimental details

$SrAlF_5$ melts congruently at 1160 K. As raw materials, SrF_2 single-crystalline pieces and AlF_3 synthesized by fluorination of pure alumina with NH_4HF_2 and separated from NH_4F by pyrolysis were used. Single crystals of $SrAlF_5$ were grown from a stoichiometric melt, in an argon–CF_4–HF mixed atmosphere by the Bridgman method, in well-closed graphite

crucibles [10]. The temperature gradient was close to 20 K cm^{-1} and the translation speed was 1 mm h^{-1}. The x-ray powder patterns of these samples were indexed with the tetragonal structure reported by Kubel ($a = 19.8755$ Å and $c = 14.3003$ Å) [22]. In addition, this lattice system was confirmed by polarized light observations and polarized Raman and infrared spectroscopy [23].

In view of the dielectric investigation, several plates oriented perpendicularly to the crystallographic axes were cut (typical surface area = 50 mm^2, thickness = 0.80 mm). Dielectric measurements were performed along the [100] and [001] directions, using an HP4192A impedance analyser in a parallel configuration (capacitance, conductance), as function of the frequency (10 Hz–10 MHz) and temperature (300–800 K). The oscillation level was kept at 1.0 V_{rms}. The experimental errors in the determination of the capacitance and conductance are almost negligible, which is evidenced by the smooth temperature dependence of the curves. Silver paste electrodes were used to connect the sample to the holders in a home-made controlled furnace under continuous linear heating/cooling rates (2.0 K min^{-1}).

3. Results

From the electrical point view, fluoride structures show high electrical conductivities at high temperatures, so that they can be classified as solid electrolytes [24–27]. In general, the high conductivity values attained at elevated temperatures come from a diffuse (or Faraday) phase transition to a fast conducting phase. The conduction mechanism is due to the appearance of defects in the structure, allowing an easy charge carrier mobility. These defects usually show an Arrhenius-type behaviour, and the ionic conductivity can be written as

$$\sigma = \frac{\sigma_0}{kT} \exp\left(-\frac{\Delta H_f/2 + \Delta H_m}{kT}\right), \tag{1}$$

where σ_0 is the conductivity at 0 K, k is Boltzmann's constant, T is the absolute temperature, and ΔH_f and ΔH_m are the charge carrier formation and migration enthalpies, respectively. In the case where more than one species are mobile, the right-hand side of equation (1) should be replaced by a sum of such terms, with the corresponding exponents and pre-factors.

In order to understand the electrical properties of $SrAlF_5$, data from complex impedance measurements of this material were analysed by means of different formalisms, such as complex conductivity ($\sigma = \sigma' + j\sigma''$) and complex permittivity ($\varepsilon = \varepsilon' + j\varepsilon''$), which are related by the Maxwell relation $\sigma = j\omega\varepsilon_0\varepsilon$, where $j = \sqrt{-1}$, ω is the angular frequency and ε_0 is the free space permissivity. Since $SrAlF_5$ belongs to a tetragonal crystalline system, only two components of the dielectric tensor are necessary to its complete characterization, namely ε'_{11} and ε'_{33}. The temperature dependence of the real part of the dielectric constant of $SrAlF_5$, between 300 and 800 K, recorded at some selected frequencies, is given in figure 1. The first feature that one can observe in this figure is a dispersive region at high temperatures ($T > 650$ K), where the magnitude of the dielectric constant decreases with the increase of the frequency of the applied electric field. This effect is still more pronounced for lower frequencies. On the other hand, below 650 K (550 K) for ε'_{11} (ε'_{33}), the real part of the dielectric constant depends linearly on the temperature and is frequency independent. At room temperature, ε'_{11} and ε'_{33} converge to 7.75 and 6.00, respectively. These values agree very well with the ones extrapolated from infrared reflectivity measurements ($\varepsilon'_{11} = 6.57$ and $\varepsilon'_{33} = 5.14$) [21]. Corresponding features occur in the real part of the electrical conductivities σ'_{11} and σ'_{33}, as shown in figure 2. A dispersive regime is observed for temperatures below 500 K, where the conductivity increases as the frequency increases. This correlation between the dielectric constant and the conductivity is in accordance with the Maxwell relation cited above.

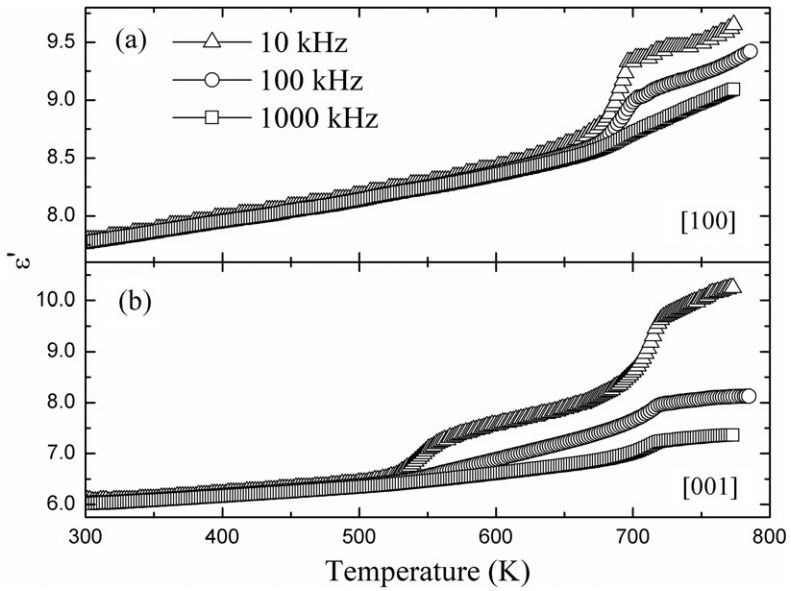

Figure 1. Temperature dependence of the dielectric constant of $SrAlF_5$ recorded in the (a) [100] and (b) [001] crystallographic directions.

Moreover, these comments fit the normal behaviour of an ionic crystal, where it is expected that for thermally activated systems the conductivity increases with raising temperatures. The reduction of the dielectric constant with the increase of the frequency can be considered as the result of relaxations originated from the ionic movement of the charge carriers among neighbour sites, which is due to the high mobility of these species under the action of an external electric field, leading to the polarization of the sample. This can be interpreted as the consequence of jump frequencies of the carriers (ions or defects): for frequencies above the characteristic jump frequency the charge carriers behave as dipole-like relaxations, bringing an additional (extrinsic) contribution to the measured conductivity. In the high-temperature region, the conductivity varies by approximately four orders of magnitude. In figures 1 and 2, one can observe the occurrence of anomalies around 700 K, which are in good agreement with those obtained using other experimental methods [18, 19, 21]. This effect will be discussed later.

Let us now investigate the frequency dispersion of σ'_{11} and σ'_{33} for some selected temperatures, presented in figure 3. The conductivity curves can be divided into two different regions, delimited by the dashed line serving as a guide for the eyes. The first region is a frequency-independent plateau (i), corresponding to the bulk *dc* conductivity σ_0. In this region, the conductivity increases with the increase of the temperature, reflecting the normal behaviour of thermally activated ionic conductors, i.e., the increase of the concentration and mobility of the charge carriers at high temperatures (the jump frequency is increased and the carriers become increasingly free). It is interesting to note that the plateau region (i) shifts from lower to higher frequencies with increasing temperatures. The second region (ii) can be observed at higher frequencies, especially for lower-temperature measurements, where the conductivity increases with frequency.

The observed behaviour of the *ac* conductivity of $SrAlF_5$ is usual for ionic conductors, and it is known as the 'universal dynamic response of dielectrics' [27, 28]. Indeed, at high

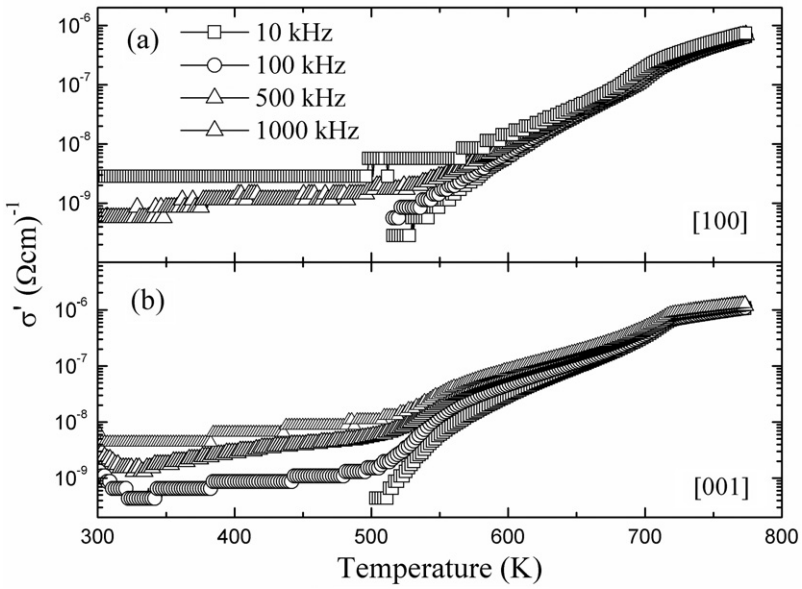

Figure 2. Temperature dependence of the electrical conductivity of $SrAlF_5$ recorded in the (a) [100] and (b) [001] crystallographic directions.

frequencies (radio regions), the electrical conductivity has a complex power-law dependence of the form $(j\omega)^n$, with $0 < n < 1$, which satisfies the Kramers–Kronig relations [29]. Then, the complex conductivity can be written as

$$\sigma(\omega) = \sigma_0 + \sigma_0 \left(\frac{j\omega}{\omega_p}\right)^n + j\omega\varepsilon_\infty, \tag{2}$$

where σ_0 is the *dc* conductivity, ω_p is the crossover frequency and ε_∞ is the high-frequency permittivity. Consequently, the real part of the conductivity can be expressed as

$$\sigma'(\omega) = \sigma_0 + \sigma_0 \left(\frac{\omega}{\omega_p}\right)^n \cos\left(\frac{n\pi}{2}\right). \tag{3}$$

The curves in figures 3(a) and (b) are the best fits of the equation (3) to the experimental data, from which the temperature dependence of the dc conductivity σ_0, the crossover frequency ω_p and the exponent n can be obtained as fitting parameters. The temperature dependence of the parameter n is shown in figure 4 in the [100] and [001] directions. For low temperatures a constant n value, close to 1, is observed in both directions. At high temperatures n_{11} and n_{33} decrease to approximately 0.8 and 0.7, respectively. These results are in good correspondence with those obtained for other crystalline materials, such as $KTaO_3:Co^{2+}$ and $CeO_2:Gd^{3+}$ [30], and may be understood on the basis of the theory that describes the hopping event as involving many-particle interactions. As a consequence, the motion of a carrier is rather influenced by the relaxation of its neighbourhood, and the exponent n is a measure of the degree of interaction [31]. In accordance with Lee *et al* [30], the limit behaviour ($n = 1$) appears to be a universal phenomenon. However, despite the large number of models presented in literature, none of them is able to completely describe the behaviour of the exponent n.

Another interesting result from our impedance spectroscopy measurements is the absence of piezoelectric resonances in the frequency dependence of both the dielectric constant and the conductivity, as can be observed in figure 3 (piezoelectric resonances usually appear as typical

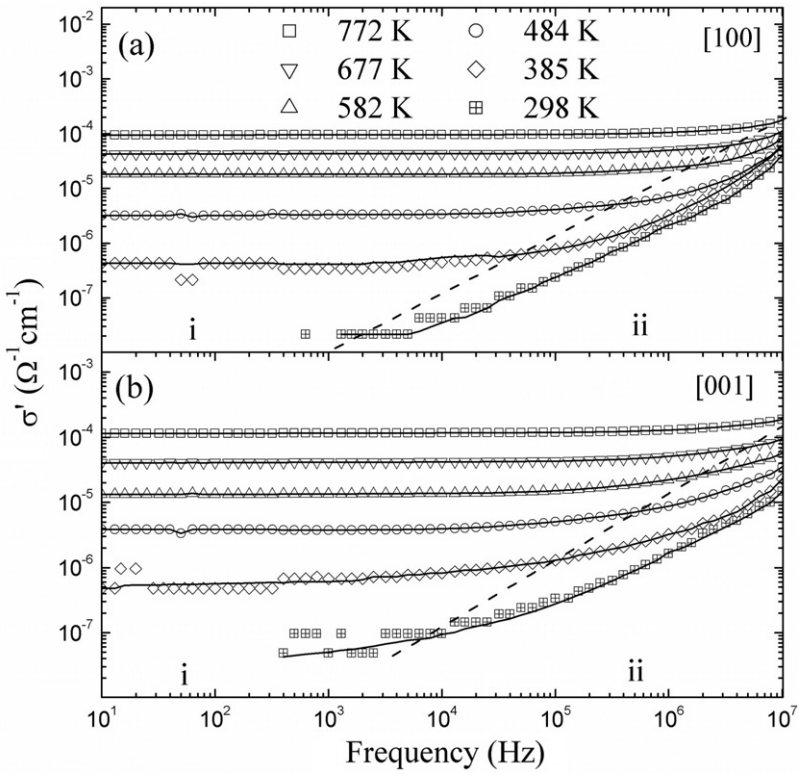

Figure 3. Frequency dependence of the electrical conductivity (a) σ'_{11} and (b) σ'_{33} of $SrAlF_5$, for selected temperatures between 298 and 772 K. The straight and dashed lines represent the best fit to equation (3) and the limits of regions (i) and (ii), respectively.

signals in the region 10^5–10^7 Hz). This result suggests the absence of a piezoelectric character in $SrAlF_5$ and should also support the hypothesis of the presence of an inversion centre in its crystalline structure.

As has been pointed out previously, the impedance spectroscopic measurements reported in this work exhibit anomalies in the real parts of the electrical conductivity and dielectric constant of $SrAlF_5$ (figures 1 and 2), which may be associated with the phase transition proposed by Abrahams and reported by other experimental techniques [19]. Since the characteristic temperature of these anomalies does not depend on the measuring frequency, in the following we will only consider the impedance data recorded at 100 kHz. Thus, in figure 5, the temperature dependence of the real part of the dielectric constant is plotted in a heating–cooling cycle, for the two main crystallographic directions. Notice that, during the heating process, the anomalies are well defined in both components, but, on cooling, an irreversible behaviour is observed, which almost completely wipes out the anomaly in the [100] direction.

In order to provide a better identification of the phase transition, we take as a criterion to identify the transition temperature (T_c) as being the temperature of the maxima of the first derivative of the experimental curves, as shown in the inset of the figure 5, for the [001] direction. Then, the phase transitions takes place at 715 K on heating and 705 K on cooling, indicating the occurrence of an appreciable thermal hysteresis. The critical temperature reported here by dielectric measurements in single crystals is in good agreement with that

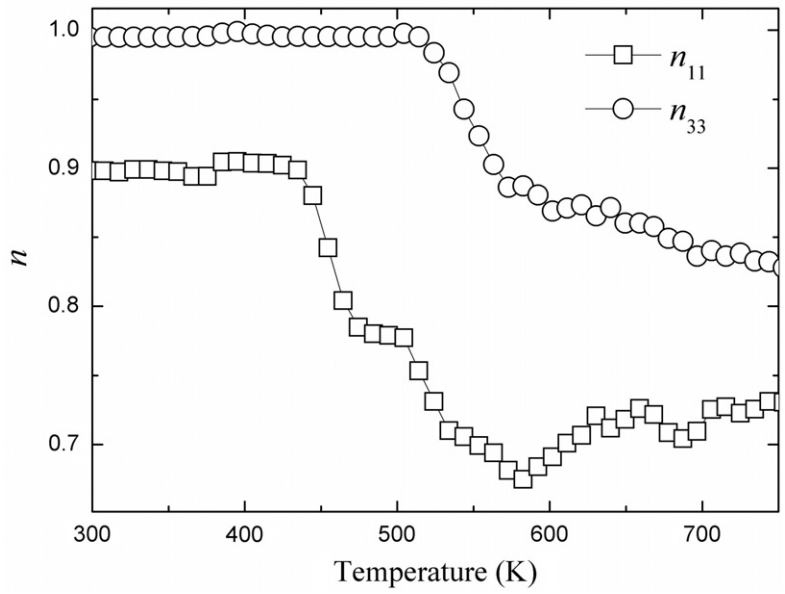

Figure 4. Temperature dependence of the n exponent, calculated from equation (3) for the [100] and [001] crystallographic directions.

observed by calorimetric and dielectric measurements in polycrystalline samples and optical birefringence in single crystals [19, 21]. The existence of a thermal hysteresis in the critical temperature indicates a first-order character for the phase transition. This result is also in accordance with the observation of a peak in the specific heat measured by Abrahams *et al* [19].

The irreversible effects in $SrAlF_5$ were first investigated performing several successive heating–cooling cycles. Figure 6 presents the temperature dependence of the electrical conductivity for two successive thermal cycles. As was previously observed in dielectric measurements, the conductivity results are characterized by an irreversible behaviour. In these cycles, one may identify three regions: (I) the heating stage below the phase transition; (II) the conductivity of the high-temperature phase; and (III) the cooling stage below the phase transition. These regions are characterized by different activation energies, which are listed in table 1, pointing to distinct dynamics of creation and diffusion of the charge carriers. As a rule, the highest activation energy is associated with the first region. On the other hand, the activation energy of the high-temperature phase is 0.90 and 0.45 eV for the [100] and [001] crystallographic directions, respectively. These activation energies may be associated with a 'molten sublattice' phase, where the charge carriers are free to move in the sublattice determined by the heavy cations. Finally, figure 6 shows that successive cycles have intermediate behaviours, indicating that the conductivity of $SrAlF_5$ is extremely dependent on the sample thermal history.

Another interesting fact to be noticed is that the activation energy of Region I is approximately the sum of those of Regions II (and I′ for the [001] direction) and III. At this point it is important to remember that the activation energy in an ionic conductor is the sum of the energies of production (mostly defect production) and diffusion of the charge carriers (see equation (1)). In a normal ionic conductor it is expected that charge carriers were created on heating and recombined on cooling. As this process is accompanied by the diffusion of such

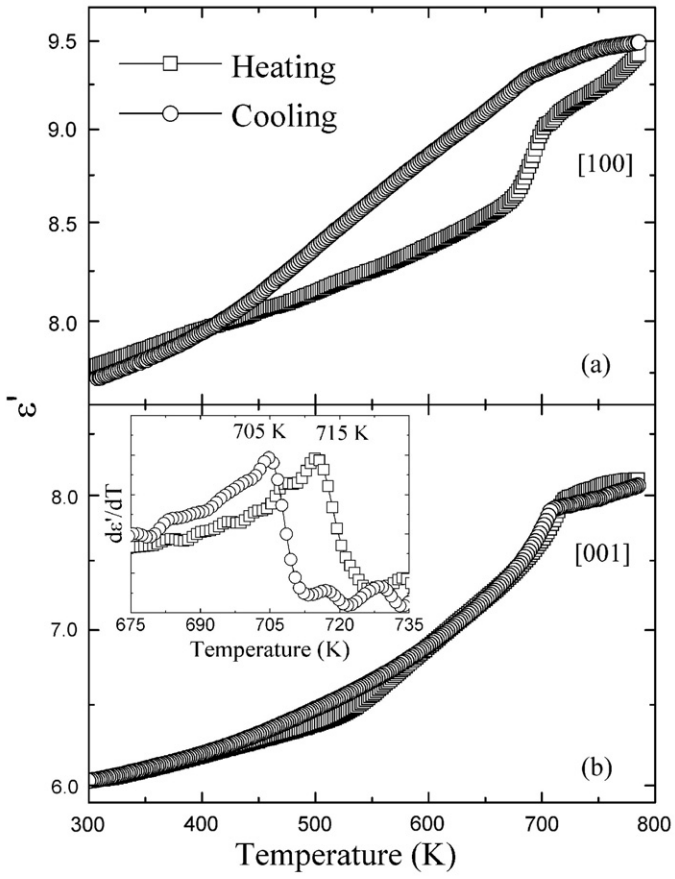

Figure 5. Temperature dependence of the dielectric constant of $SrAlF_5$ in (a) the [100] direction and (b) the [001] direction in a heating–cooling cycle, recorded at 100 kHz. The inset shows the derivative of ε'_{33} as a function of temperature in the phase transition region.

Table 1. Activation energies of the different regions of the conductivity data of $SrAlF_5$.

Region	ΔE_a^{11} (eV)	ΔE_a^{33} (eV)
I	1.08(1)	1.40(5)
I′	—	0.67(1)
II	0.90(1)	0.45(1)
III	0.20(1)	0.40(1)

species, usually it is not possible to separate both effects in a simple conductivity measurement. In our case, the irreversible behaviour suggests that some kind of defects still contribute to maintaining a high number of charge carriers at low temperatures, giving rise to an appreciable ionic conductivity below 500 K. The origin of these low-temperature defects may be explained by at least two mechanisms. On the one hand, it should correspond to a net loss of fluorine ions in the sample due to the reaction with water vapour at high temperatures. As this is a well known effect in fluoride crystals, we protected our crystals by performing all the measurements in a dry nitrogen atmosphere. On the other hand, and considering the complexity of the $SrAlF_5$

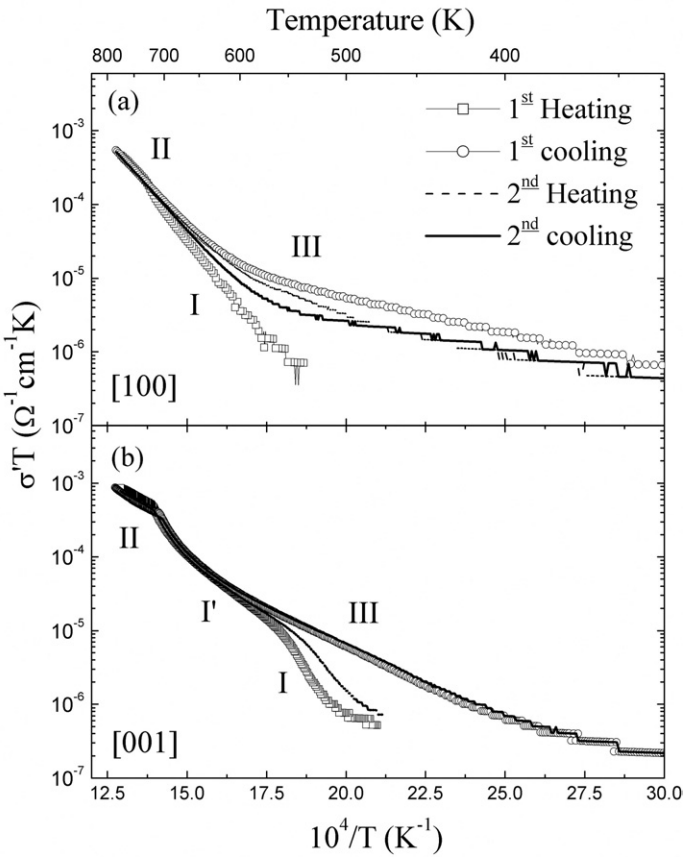

Figure 6. Arrhenius plots of two heating–cooling cycles of the electrical conductivity of $SrAlF_5$, recorded at 100 kHz, in the (a) [100] and (b) [001] directions.

crystalline structure, the low-temperature charge carriers may be associated with metastable defect configurations, with a slow recombination dynamics, for which the cooling rate used is too fast to allow them to reach the stable configuration. The main difference between these two mechanisms lies in the fact that, after some characteristic time, the recombination of the vacancies considered by the second mechanism should recover the original state, whereas the first mechanism is associated with a completely irreversible process.

In order to investigate the origin of the conductivity irreversibilities, on the basis of the models discussed above, a heating–cooling cycle was performed in a [100] sample, but the cooling process was interrupted by two isothermal stages. The first isotherm took place at 672 K, where the electrical conductivity was measured during 48 h. After that, we continued the cooling run down to 470 K and, again, we recorded the electrical conductivity for approximately 48 h. Finally, a new heating–cooling cycle was performed without any interruption. The temperature dependence of the conductivity through these cycles is presented in figure 7. The temperature of the first isotherm was chosen in order to lie in the region where the electric conductivity is independent of the sample thermal history. As could be expected, no appreciable changes in the conductivity were observed after 48 h at 672 K. On the other hand, the conductivity exhibited a strong fall as a result of the second isotherm, i.e., after 48 h at 470 K. Note that in this isotherm the trend is the lowering of the conductivity

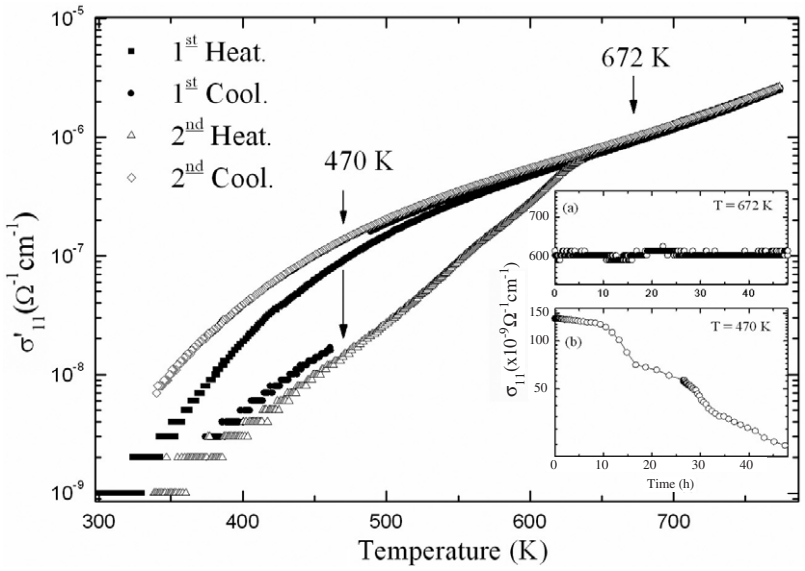

Figure 7. Temperature dependence of the [100] conductivity of $SrAlF_5$ in two thermal cycles. The inset shows the time dependence of the conductivity in two isotherms at (a) 672 K and (b) 470 K, as described in the text.

towards the value observed in the first heating. This result supports the idea that the observed irreversibility is associated with metastable states. For these states the cooling rate used in this work (2 K min^{-1}) is not slow enough to allow the system to evolve through quasi-stationary states. The adequate cooling rates should be estimated by analysing the temporal evolution of the conductivity along the isotherms, which are shown in the inset of the figure 7. As discussed above, the conductivity remained constant during the 48 h, when the temperature was held at 672 K (inset (a)). This result indicates that above approximately 630 K, the characteristic relaxation times are very small and the conductivity does not depend on the cooling rate. On the other hand, the second isotherm (inset (b)) exhibits a very complex behaviour, where it is possible to identify several relaxation processes, probably associated with different metastable states with different relaxation times. After 48 h, although the conductivity relaxed by almost one order of magnitude, the system did not reach the stationary state, indicating that extremely slow relaxation processes are present. After the end of this first cycle, where the system was allowed to relax, the second thermal cycle recovered the behaviour of a virgin sample, exhibiting the three characteristic regions described in figure 6. Notice that the recovering of the original state also contributes to ruling out the hypothesis of sample degradation, since there is no fluorine source to recombine the vacancies that should be originated in such a process. Once these experiments prove that the observed irreversibility is associated with some kind of metastable processes, we may assume that the excess of charge carriers has its origin in the inhibition of the recombination of charged defects produced during the heating process. Thus, a detailed analysis of the different types of defect and their diffusion processes would be of great importance for understanding the conduction process in $SrAlF_5$.

4. Discussion

In order to discuss the possible conduction mechanisms of fluorine ions in $SrAlF_5$, we first need to make some considerations regarding its crystalline structure. In a recent paper a

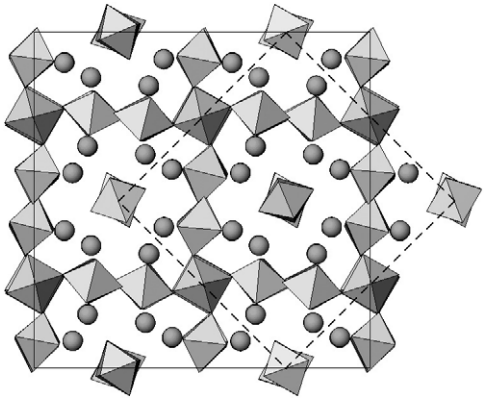

Figure 8. Crystalline structure of $SrAlF_5$ according to Kubel [22] projected in the *ab*-plane. The dashed line represents the reduced unit cell associated with the $BaTiF_5$ structure [32]. Spheres stand for strontium atoms. Fluorine atoms are placed at the corners of the octahedra.

comparison of the reported crystalline structures for $SrAlF_5$ was carried out on the basis of the optical phonon spectra [23]. The results support the hypothesis of a centrosymmetric tetragonal body-centred lattice being possibly a superstructure of the $I4/m$ space group, as reported by Kubel [22], and closely related to that of other members of the ABF_5 family (see figure 8). These structures are composed basically of networks of BF_6 (B = Al, Ti) octahedra, oriented parallel and perpendicular to the crystalline axes, and cations (A = Sr, Ba) occupying the interstices among these octahedra. The main difference between the structures of the ABF_5 family is due to the octahedra at the corners and centre of the reduced cell (dashed line in figure 8). According to Kubel [22], in the case of $SrAlF_5$ these octahedra are unconnected, giving rise to dimers (Al_2F_{10}) aligned along the z-axis, but consecutive dimers are rotated by 90° due to the screw axis present in this structure. On the other hand, in $BaTiF_5$ [32] the number of fluorine sites in these dimers is doubled and all of them are half-occupied, corresponding to a disordered configuration of the Al_2F_{10} dimers.

Since $SrAlF_5$ has a well packed structure and no tunnels are available for the diffusion of interstitial anions, one may assume that the conduction process is mainly due to the diffusion of fluorine vacancies through regular atomic positions. Considering the reported structure of $SrAlF_5$, one may notice that the F–F interatomic distances associated with the simplest diffusion pathways are very close (2.5–3 Å), suggesting that any diffusion mechanism is strongly privileged from a geometric point of view. Indeed, this idea agrees with the close values of the conductivity in both crystallographic directions (figure 2). The fact that the shortest F–F distance (2.5 Å) corresponds to the corner-sharing octahedra chains aligned along the z-axis should address the slightly higher conductivity in this direction. The large number of fluorine sites available for hosting vacancies suggests that several processes may be thermally activated, depending on the temperature of the sample, originating the complex behaviour observed in the Arrhenius plots of the figure 6.

Even though there are no conclusive evidences in favour or against the ferroelectric character of $SrAlF_5$, the existence of a high-temperature phase transition was verified by several experimental techniques. By considering the conductivity results presented in this work and the crystalline structures of the ABF_5 family, one may suggest that the anomalies observed at ∼710 K in $SrAlF_5$ are associated with an order–disorder phase transition ($I4_1/a \rightarrow I4/m$) involving the Al_2F_{10} dimers. Thus, after this transformation a large number of additional

fluorine vacancies is introduced in the structure, which also reduces the intra- and inter-dimer F–F distances to ∼2 Å. Such an increase in the available number of charge carriers allows this compound to have a similar behaviour to that of a molten-lattice superionic conductor. However, since only part of the fluorine sublattice is involved in this process, the electrical conductivity does not reach the levels of a superionic conductor. Furthermore, the cage-like configuration of the column of dimers, which are surrounded by strontium cations, favours the existence of metastable states, since a rapid cooling rate would 'freeze' some fluorine anions in the interstitial sites between the dimers, maintaining a similar arrangement to that of the high-temperature phase. Depending on the characteristic relaxation times of these anions, they would recombine with vacancies of the different groups of octahedra, giving rise to the complex temporal evolution observed in the measured isotherms (figure 7). Even though the proposed models are capable of giving a qualitative image of the mechanisms involved in the conduction processes and in the phase transition, high-temperature structural investigations and computational simulations are necessary to obtain a better description of the transport properties of $SrAlF_5$.

5. Conclusions

In this work we investigated the electrical and dielectric properties of $SrAlF_5$, as functions of frequency and temperature. Our results show that the frequency dependence of the electrical conductivity follows a power-law behaviour with exponents decreasing as the temperature increases and ranging from $0.7 < n_{[100]} < 0.9$ and $0.8 < n_{[001]} < 1$. The existence of a phase transition around 715 K, with a thermal hysteresis of 10 K, was verified in both the conductivity and the dielectric constant. $SrAlF_5$ exhibits the classic behaviour of an ionic conductor, with activation energies varying between 0.2 and 1.40 eV. The conduction process appeared to be dependent on the sample thermal history, but the isothermic time evolution of the conductivity showed that this effect is associated with metastable states. A detailed analysis of the possible conduction pathways based on the crystalline structure of $SrAlF_5$ and other members of the ABF_5 family suggests that the phase transition would have an order–disorder character and the metastable states would correspond to defects trapped in the columns of Al_2F_{10} dimers.

Acknowledgments

This work was partially supported by the Brazilian government agencies CNPq, CAPES, FUNCAP and FAPEMIG. The authors thank Dr M E G Valerio for helpful discussions.

References

[1] Lai S T, Jenssen H P and Gabbe D 1985 *J. Opt. Soc. Am.* A **2** 44
[2] Dubinskii M A, Schepler K L, Semashko V V, Abdulsabirov R Y, Korableva S L and Naumov A K 1998 *J. Mod. Opt.* **45** 221
[3] Jenssen H P and Lai S T 1986 *J. Opt. Soc. Am.* B **3** 115
[4] Wang D M, Hutton D R, Troup G J and Jenssen H P 1986 *Phys. Status Solidi* a **98** K73
[5] Andrade A A, Tenorio E, Catunda T, Baesso M L, Cassanho A and Jenssen H P 1999 *J. Opt. Soc. Am.* B **16** 395
[6] Vink A P, Dorenbos P, de Haas J T M, Donker H, Rodnyi P A, Avanesov A G and van Eijk C W E 2002 *J. Phys.: Condens. Matter* **14** 8889
[7] Rodnyi P A, Mikhrin S B, Dorenbos P, van der Kolk E, van Eijk C W E, Vink A P and Avanesov A G 2002 *Opt. Commun.* **204** 237
[8] Hewes R A and Hoffman M V 1971 *J. Lumin.* **3** 261
[9] Hoffman M V 1971 *J. Electrochem. Soc.* **118** 933

[10] Meehan J P and Wilson E J 1972 *J. Cryst. Growth* **15** 141
[11] van der Kolk E, Dorenbos P, van Eijk C W E, Vink A P, Weil M and Chaminade J P 2004 *J. Appl. Phys.* **95** 7867
[12] Shimamura K, Víllora E G, Muramatsu K and Ichinose N 2005 *J. Cryst. Growth* **275** 128
[13] Víllora E G, Shimamura K, Muramatsu K, Takekawa S, Kitamura K and Ichinose N 2005 *J. Cryst. Growth* **275** 145
[14] Ravez J 1997 *J. Physique* III **7** 1129
[15] Abrahams S C and Ravez J 1992 *Ferroelectrics* **135** 21
[16] Ravez J 2000 *C. R. Acad. Sci.* IIC **3** 267
[17] Abrahams S C, Kurtz S K and Jamieson P B 1968 *Phys. Rev.* **172** 551
[18] Ravez J, Abrahams S C, Chaminade J P, Simon A, Grannec J and Hagenmuller P 1981 *Ferroelectrics* **38** 773
[19] Abrahams S C, Ravez J, Simon A and Chaminade J P 1981 *J. Appl. Phys.* **52** 4740
[20] von der Mühll R, Andersson S and Galy J 1971 *Acta Crystallogr.* B **27** 2345
[21] Canouet S, Ravez J and Hagenmuller P 1985 *J. Fluorine Chem.* **27** 241
[22] Kubel F 1998 *Z. Anorg. Allg. Chem.* **624** 1481
[23] Silva E N, Ayala A P, Mendes Filho J, Moreira R L and Gesland J Y 2004 *J. Phys.: Condens. Matter* **16** 7511
[24] Uvarov N F and Hairetdinov E F 1989 *Solid State Ion.* **36** 29
[25] Toshmatov A D, Aukhadeev F L, Terpilovskii D N, Dudkin V A, Zhdanov R S and Yagudin S I 1988 *Sov. Phys.—Solid State* **30** 111
[26] Chandra S 1981 *Superionic Solids-Principles and Applications* (Amsterdam: North-Holland)
[27] Beyeler H U, Bruesch P, Pietronero L, Schneider W R, Strassler S and Zeler H R 1979 *Physics of Superionic Conductors* ed M B Salamon (New York: Springer)
[28] Jonscher A K 1977 *Nature* **267** 673
[29] Funke K 1993 *Prog. Solid State Chem.* **22** 111
[30] Lee W K, Liu J F and Nowick A S 1991 *Phys. Rev. Lett.* **67** 1559
[31] Maass P, Petersen J, Bunde A, Dieterich W and Roman H E 1991 *Phys. Rev. Lett.* **66** 52
[32] Eicher S M and Greedan J E 1984 *J. Solid State Chem.* **52** 12